

ISONIAZID-BASED SCHIFF'S BASES IN BONE CANCER STUDIES USING MG-63 CELL LINES

G. MUNI HEMALATHA^{1,2}, KANDASAMY THIRUNAVUKKARASU^{1*}, C. RAMESH KUMAR³

¹Vel Tech Rangarajan Dr. Sagunthala R and D Institute of Science and Technology, Chennai 600062, India, ²Sree Vidyanikethan Degree College, Affiliated to Sri Venkateswara University, Tirupathi, India, ³Department of Chemistry, Madras Christian College (Autonomous), University of Madras, Chennai 600059, India
*Email: kthirunavukkarasu@gmail.com

Received: 18 Apr 2021, Revised and Accepted: 27 May 2022

ABSTRACT

Objective: Anticancer activities of Schiff bases S1 and S2 against MG-63 human osteosarcoma cells were performed and described using an *in vitro* evaluation employing cytotoxicity and apoptosis assay.

Methods: MG-63 cells were used in an MTT assay to examine the effect of the compound on cell viability (S1 and S2). Cell morphologies and IC50 values were obtained. The acridine orange (AO)/ethidium bromide (EB) dual staining technique was used to determine the apoptosis process.

Results: Our findings showed that synthesised S1 and S2 reduced MG-63 cell proliferation and induced apoptosis in a dose-dependent manner, implying that they could be used to treat bone cancer.

Conclusion: Our findings showed that synthesised S1 and S2 reduced MG-63 cell proliferation and induced apoptosis in a dose-dependent manner, implying that they could be used to treat bone cancer.

Keywords: Isoniazid, Inhibitory zone, MG63 cell lines, Carcinoma, Osteosarcoma cells, Cytotoxicity, Apoptosis assay, Dual staining

© 2022 The Authors. Published by Innovare Academic Sciences Pvt Ltd. This is an open access article under the CCBY license (<https://creativecommons.org/licenses/by/4.0/>) DOI: <https://dx.doi.org/10.22159/ijap.2022.v14i.48> Journal homepage: <https://innovareacademics.in/journals/index.php/ijap>

INTRODUCTION

Cancer, one of the complex diseases, thrives in a heterogeneous and adaptive environment [1-10]. Bones are affected as a common consequence in metastatic cancer patients with multiple myeloma, breast, prostate, primary colon, lung, and kidney tumors [11, 12]. Ewing sarcoma (ES), Osteosarcoma (OS), and chondrosarcoma (CS) are the most prevalent primary malignant bone tumors, accounting for over 70% of all malignancies [13]. Out of the above three, osteosarcoma is a type of cancer that is more common in children and adults, with the lungs being the most common site of metastasis in more than 80% of patients [10, 14, 15]. The annual incidence of osteosarcoma is 2-3 million/year in the general population, but in adolescence, it is higher, where it shows 8-11 million/year at later adolescent age (15-19 y) and affects with 15% of all solid extracranial malignancies in this age group. Males are 1.4 times more likely than females to be impacted [16, 17]. Patients with osteosarcoma who undergo surgical treatment have a long-term survival rate of 20-30 percent [18]. Moreover, osteosarcoma is a highly metastatic, aggressive, and lytic tumor that frequently metastasizes to the human lung [19]. The presence of malignant mesenchymal cells creating osteoid and/or immature bone characterizes osteosarcoma, the most common primary solid cancer of bone [20-22]. Even though adjuvant chemotherapy has improved the treatment of osteosarcoma to some extent, it remained virtually unchanged over the last thirty years, probably because of chemotherapeutic resistance [23]. Hence new osteosarcoma treatment techniques are desperately needed.

The Schiff base reaction occurs when aldehydes (or ketones) combine with amino acids, forming imine groups (C=N). Schiff bases of heterocyclic aldehydes and amino acids containing nitrogen, oxygen, and sulphur atoms are a class of compounds that exhibit significant biological activity [24], including antiviral [25], antifungal [26], antioxidant [27], anti-inflammatory [28], antitumor [29, 30], anticancer [31, 32], antibacterial [33, 34], and antipyretic applications [11, 35]. Several biological activities such as cytotoxicity studies, antibacterial, antifungal, anti-tuberculosis, DNA binding, antioxidant, scavenging, and antiviral activities have been performed [36] using isoniazid Schiff bases. Isoniazid Schiff bases, formed by the reaction of Isonicotinohydrazide and a corresponding heterocyclic carbaldehyde, have a pyridine ring and a hydrazide

group, which contains the characteristic HC=N-NH-C=O group. This group leads to intermolecular and intramolecular hydrogen bonding, which increases greater biological activities because of strong interactions with the binding sites of the target tumor cells [37]. Indeed, isoniazid derivatives were subjected to extensive research in tuberculosis treatment in recent decades [38, 39]. But this drug was rarely investigated in the field of cancer treatment [37, 40, 41].

Berkesi *et al.* studied some Schiff bases and found that (E)-2-hydroxy Benzaldehyde-N-phenyl imine and (E)-Benzaldehyde-N-2-hydroxy phenyl imine exhibited intramolecular hydrogen bonding in solid-state as well as in solution and thereby decided the geometry [42]. Yong *et al.* studied anti-bacterial activities for a few selected bacterial strains for different isoniazid Schiff base derivatives and found that the Schiff base derivative in which the carbaldehyde group was present in the ortho position to a heterocyclic ring was more active than others [43]. Rodrigues *et al.* studied the cytotoxicity activity of some isoniazid derivatives against human ovary, glioblastoma and colon cancer cells [44]. They found that the presence of hydroxyl group on the aldehyde containing ring exhibited a significant role in the anticancer activities of a series of isoniazid derivatives, especially when it was located in ortho-position. Generally, anticancer studies are conducted using cancer cell lines which leads to apoptosis, a programmed cell death.

Apoptosis is a form of genetically controlled programmed cell death that regulates the evolution of multicellular organisms and tissues by removing physiologically redundant, physically damaged, and defective cells [45]. Under a fluorescent microscope, dual acridine orange (AO)/ethidium bromide (EB) fluorescence labelling may be used to study membrane changes linked with apoptosis [5, 46]. Additionally, this approach is capable of properly identifying cells at various phases of apoptosis [47-49]. A number of isonicotinoyl hydrazones were tested for their cytotoxicity against A549 human lung cancer cells [50], as well as the manner of cell death, which was shown to be apoptotic using several staining methods [1].

In this work, we synthesized isoniazid-based cation receptor Schiff bases (E)-N'-((1H-Pyrrol-2-yl) methylene) isonicotinohydrazide (S1) and (E)-N'-(thiophen-2-yl-methylene) isonicotinohydrazide (S2) supported heterocyclic derivatives by mechanical grinding followed by condensation reaction between their corresponding heterocyclic

aldehydes. Their structures were established by ^1H NMR, ^{13}C NMR, and FT-IR. As these are active against bone cancer, MTT assay was done and IC50 values were procured and cell morphologies were identified. AO/EB dual staining was done by which apoptosis of cells were identified under fluorescent microscope with specified magnifications. The synthesized drugs were cheaper in cost and helps in apoptosis of bone cancer cells [2].

MATERIALS AND METHODS

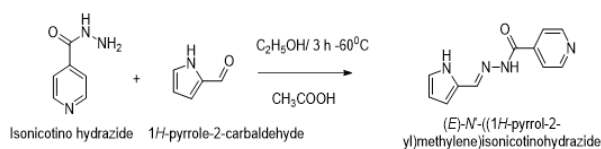
Materials

All the solvents and chemicals used in the present work were of analytical (AR or GR) grade (Sigma Aldrich) and used without any further purification. Isoniazid, pyrrole-2-carboxaldehyde, thiophene-2-carboxaldehyde, acetic acid, acridine orange (AO), ethidium bromide (EB), 3-(4,5-dimethylthiazol-2-yl)-2,5-diphenyltetrazolium bromide (MTT), DMSO, PBS (1%), Dulbecco's Modified Eagle Media (DMEM), 10% FBS (Fetal Bovine Serum), Penicillin, streptomycin.

Methods

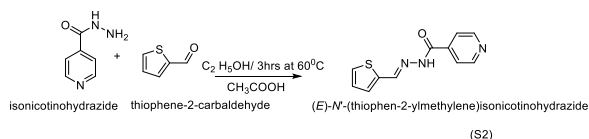
Synthesis of (E)-N'-((1H-Pyrrol-2-yl) methylene) isonicotinohydrazide (S1):

Receptor S1 was synthesized in a single step by the condensation reaction of equimolar amounts of isoniazid (5 mmol=686 mg) and pyrrole-2-carboxaldehyde (5 mmol=475 mg) with 10 ml of ethanol in presence of 1-2 drops of acetic acid and is heated at 60 °C for 3 h. Re-crystallisation is done with ethanol. Further purification is checked with the TLC technique. The receptor (S1) formed is amorphous powder, which is yellow in color. Its melting point is 217-219 °C.



Synthesis of (E)-N'-(thiophen-2-ylmethylene) isonicotinohydrazide (S2)

Receptor S2 was synthesized in a single step by the condensation reaction of equimolar amounts of isoniazid (5 mmol=686 mg) and Thiophene-2-carboxaldehyde (5 mmol=617 mg) with 10 ml of ethanol in the presence of 1-2 drops of glacial acetic acid and is heated at 60 °C for 3 h. Re-crystallisation is done with ethanol. Further purification is checked with the TLC technique. The receptor (S2) formed is amorphous powder, which is light yellow in color. Its melting point is 256-257 °C.



Anti-cancer activity

From the cell repository of the National Centre for Cell Sciences (NCCS), Pune, India, human cell lines were procured. For maintaining the cell line, we utilized Dulbecco's Modified Eagle Media (DMEM) (Christiya *et al.*, 2021), which was provided with 10% FBS (Fetal Bovine Serum). To prevent the medium from bacterial contamination penicillin (100U/ml) and streptomycin (100µg/ml) were added and a humidified environment with 5% CO₂ at 37 °C was maintained.

Cell cytotoxicity (MTT assay)

The cytotoxicity of S1 and S2 on MG-63 cells was determined by the method of Mosmann [51]. In cell viability assay, MG-63 visible cells were harvested and were counted using a hemocytometer and diluted in Dulbecco's Modified Eagle Media (DMEM) to a density of 1×10^4 cells/ml and were seeded in 96 well plates for every well and allowed for attachment. After 24h of incubation, it had been treated with control and with S1 and S2 at various concentrations (5, 10, 15,

20, 25, 30, 35, and 40 µg/well), which are incubated at 37 °C during a humidified 95% air and 5% CO₂ incubator for twenty-four hours. After incubation, the drug-containing cells were washed with a fresh culture medium, and each well was incubated for an additional 4 h at 37 °C with 5 mg/ml MTT in PBS. MTT (bromide of 3-(4,5-dimethylthiazol-2-yl)-2,5-diphenyltetrazolium) is reduced in living cells by mitochondrial dehydrogenase, generating a purple colour that may be seen. In live cells, NAD (P) H-dependent reductase transforms the MTT reagent into the purple-colored formazan [3]. The precipitate was dissolved in 100 ml DMSO, and cell viability was followed at 540 nm with a multi-well plate reader. The results were expressed as a percentage of stable cells relative to the control group. The half-maximal inhibitory concentration (IC-50) values were estimated, and optimum doses were then determined at different base amounts [34].

$$\text{Inhibitory of cell proliferation (\%)} = \frac{\text{Mean absorbance of the control} - \text{Mean absorbance of the sample} \times 10}{\text{Mean absorbance of the control}}$$

The IC50 values were obtained using the S1 and S2 dose-response curves, which demonstrated a 50% suppression of cytotoxicity relative to vehicle control cells. All experiments have been repeated a minimum of three times [3].

Dual labelling with acridine orange and ethidium bromide (AO/EB) to quantify apoptotic induction: The microscopic fluorescence study of apoptotic necrobiosis was performed in accordance with Baskic *et al.* approach [51].

In a very 6 well plate 5×10^4 cells/well of MG-63 cells were seeded and incubated for 24 h. After 24 h of S1 and S2 treatment, the cells were detached, washed with cold PBS, and stained for 5 min at room temperature with a combination of AO (100g ml⁻¹) and EB (100g ml⁻¹) (1:1). At magnifications of 40x and 20x, the stained cells were examined using a fluorescence microscope (S1 and S2). At the conclusion of the treatment, the cells were collected and washed three times with PBS. After 5 min of staining with acridine orange/ethidium bromide (AO/EB 1:1 ratio; 100g/ml), the plates were immediately inspected at magnifications of 40x (S1) and 20x (S2) using a fluorescence microscope (S2). The number of apoptotic cells was estimated as a function of the total number of cells in the field [58].

RESULTS

For (E)-N'-((1H-Pyrrol-2-yl) methylene) isonicotinohydrazide (S1)

Fourier transformation Infrared Spectroscopy (FT-IR)

IR spectra was taken using Agilent Resolutions Pro. The complex indicated bands due to $\text{C}=\text{O}$ stretching of amide at 1756 cm^{-1} , N-H stretching of secondary amide at 3210 cm^{-1} , N-H stretching of secondary amine at 3449 cm^{-1} , aromatic CH stretching at 3064 cm^{-1} , $\text{C}=\text{C}$ stretching of aromatic ring at 1605 cm^{-1} , 1494 cm^{-1} , 1442 cm^{-1} , 912 cm^{-1} to 686 cm^{-1} due to CH-bend of aromatic ring, $\text{SP}^2\text{-CH}$ stretch at 3140 cm^{-1} and $\text{C}=\text{N}$ stretch at 1642 cm^{-1} .

The ^1H NMR spectral data of the ligand S1 is matching with the literature reports.

^{13}C : The ^{13}C NMR data of the complex were recorded using DMSO as an internal standard. Signals received at 162.2, 150.2, 141.4, 140.0, 127.2, 122.8, 121.7, 114.8, 109.6.

For (E)-N'-(thiophen-2-ylmethylene) isonicotinohydrazide (S2)

Fourier Transformation Infrared Spectroscopy (FT-IR):

IR spectra was obtained using Agilent Resolutions Pro. The complex indicated bands due to $\text{C}=\text{O}$ stretching at 1659 cm^{-1} and N-H stretch of amide at 3203 cm^{-1} , C-H stretch of aromatic at 3021 cm^{-1} , $\text{C}=\text{C}$ stretch of aromatic ring at 1575 cm^{-1} , 1412 cm^{-1} , C-H bending of aromatic at 846, mono substituted aromatic ring at 748 cm^{-1} , 680 cm^{-1} , $\text{C}-\text{N}$ stretch at 1042 cm^{-1} , 1154 cm^{-1} , 1292 cm^{-1}

The ^1H NMR spectral data of the ligand S2 is matching with the literature.

^{13}C : The ^{13}C NMR data of the complex were recorded using DMSO as an internal standard. It indicated signals at 161.9, 150.8, 144.6, 140.9, 139.3, 131.9, 129.8, 128.4, 122.0.

Cell Cytotoxicity: (MTT assay)

The MG-63 cell viability with various concentrations of S1 and S2 were tabulated in table 1 and 2. A plot was drawn between the calculated % of cell cytotoxicity or viability against the different concentrations of

S1/S2, and half-maximal inhibitory concentration (IC-50) was noted (fig. 1 and 2). The fluorescent microscope was used to investigate the vitality and cytological features of MG-63 cells (fig. 1). Increased S1 and S2 concentrations drastically reduced the number of viable osteosarcoma cells and disrupted their structure [3, 6].

Table 1: MTT assay–bone cancer MG63 cells of (E)-N'-((1H-Pyrrol-2-yl) methylene) isonicotinohydrazide (S1)

MTT assay									
Conc	Control	5 µg	10 µg	15 µg	20 µg	25 µg	30 µg	35 µg	40 µg
Mean	109	106.66	97.61	83.17	69.87	58.71	45.27	33.2	29.2
	91	89.04	81.49	69.43	58.33	49.01	37.79	27.72	24.38
	100.1	97.95	89.64	76.38	64.16	53.91	41.57	30.49	26.82
Avg	100.03	97.88	89.58	76.32	64.12	53.87	41.54	30.47	26.8
SD	9.00	8.81	8.06	6.87	5.77	4.85	3.74	2.74	2.41

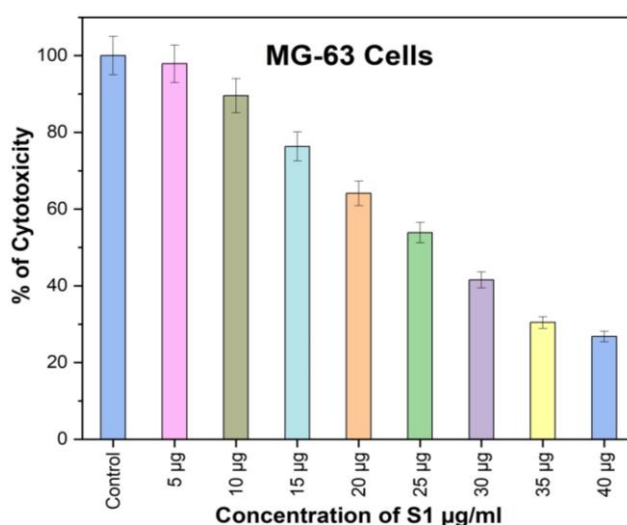


Fig. 1: Effect of compounds on cell viability determined by MTT-assay with MG-63 cells with increasing concentrations (5-40 µg/ml) of compound S1

Table 2: MTT assay–bone cancer MG63 cells of (E)-N'-(thiophen-2-ylmethylene) isonicotinohydrazide (S2)

MTT assay									
Conc	Control	5 µg	10 µg	15 µg	20 µg	25 µg	30 µg	35 µg	40 µg
Mean	100	94.11	86.23	79.31	69.36	69.74	57.81	44.83	38.71
	100	93.27	81.09	72.91	70.03	59.59	51.73	47.23	31.82
	99.9	97.32	87.53	81.38	75.09	61.37	59.08	41.08	33.09
Avg	99.96	94.83	83.23	78.31	71.49	63.56	56.20	44.38	34.54
SD	0.05	2.13	2.91	3.61	2.55	4.42	3.20	2.53	2.99

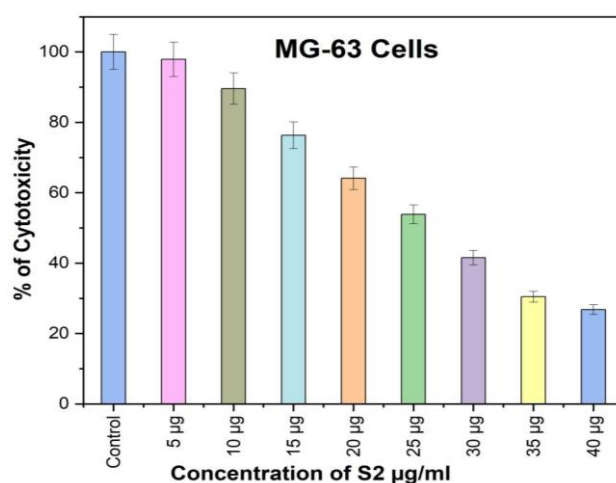


Fig. 2: Effect of compounds on cell viability determined by MTT assay with MG-63 cells with increasing concentrations (5-40 µg/ml) of compound S2

From the MTT assay by the values obtained from table 1, by plotting a graph between an increase in concentrations on the X-axis and (avg) percent of cytotoxicity on the Y-axis, it was determined that cell viability decreased significantly to 98%, 89%, 76%, 64%, and 54% when cells were exposed to MG-63 at concentrations of 5, 10, 15, 20, and 25 µg/ml, respectively [56]. 50% viable cells were observed at 26.5 µg/ml on MG-63 cells after 24 h. S1's IC50 value was determined to be 26.5 µg/ml based on this finding. MG-63 cell viability decreased drastically in a concentration-dependent manner, with an IC50 of 26.5 µg/ml (the concentration that inhibits growth by 50 percent [3] (fig. 1). Cells exceeding 40 µg/ml are completely destroyed (p0.05). In cells treated with a 40 µg/ml concentration of S1, a change in cell shape was seen along with a drop in cell quantity [7].

On the other hand, based on the MTT assay results from table 2, plotting a graph between the increase in concentrations on the X-axis and the (avg) percentage of cytotoxicity on the Y-axis indicated that cell viability was considerably decreased to 95, 83, 78, 71, 63, and 56 percent, when cells were exposed to MG-63 at concentrations

of 5, 10, 15, 20, 25, and 30 µg/ml. At 33.7 µg/ml, 50% of viable cells were found on MG-63 cells after 24 h. The IC50 values for (E)-N'-(thiophen-2-ylmethylene) isonicotinohydrazide (S2) were determined to be 33.7 µg/ml based on this finding. MG-63 cell survival decreased drastically in a dose-dependent manner, with an IC50 of 33.7 µg/ml (the concentration that inhibits growth by 50 percent (fig. 4). Cells exceeding 40 µg/ml are completely destroyed (p 0.05). In cells treated with a 40 µg/ml concentration of (E)-N'-(thiophen-2-ylmethylene) isonicotino hydrazide, a change in cell shape was seen along with a drop in cell number (S2) [7].

Effect of S1 and S2 on cell morphology

S1 and S2 produced structural changes in MG-63 cells, as indicated by microscopy. At 40x magnification, the photomicrograph demonstrates the morphological changes in MG-63 cells induced by S1, including shrinkage, detachment, membrane blebbing, and distorted shape, as a result of treatment with S1 (20 and 26.50 µg/ml for 24 h). Using a light microscope, the control cells displayed normal intact cell morphology [3] (fig. 3).

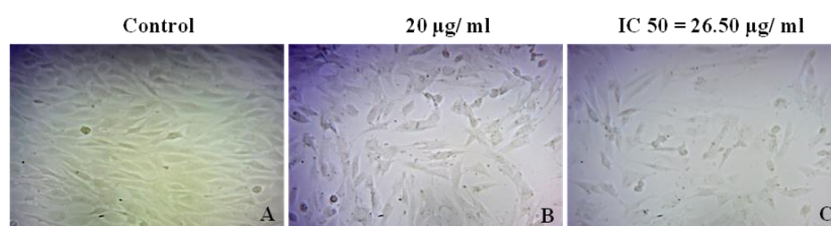


Fig. 3: Changes in morphology in control and S1 treated bone marrow MG-63 cells for 24 h. A) control, B) 20 µg/ml, C) IC 50

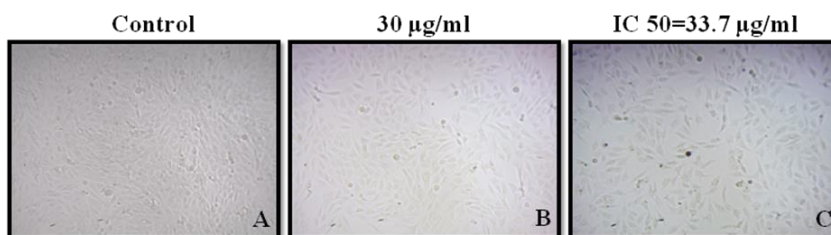


Fig. 4: Changes in morphology in control and S2 treated bone marrow MG-63 cells for 24 h. A) control, B) 20 µg/ml, C) IC 50

The photomicrograph at 20x shows the morphological alterations in MG-63 cells caused by sample (E)-N'-(thiophen-2-ylmethylene) isonicotinohydrazide (S2) treatment (30 and 33.7 µg/ml for 24 h). The control cells exhibited typical intact morphology and were imaged using a light microscope [3] (fig. 4).

Apoptosis Induction in MG-63 cells by S1 and S2 stained with AO/EB

Human osteosarcoma cells treated with S1 (20 and 26.50 µg/ml) for 24 h and S2 (30 and 33.7 µg/ml) for 24 h, stained with dual dye AO/EB and analyzed by fluorescence microscopy at 40x and 20x magnification.

Acridine orange is permeable and staining all viable/non-viable MG-63 cells. If it is intercalated into a double-stranded nucleic acid

(DNA), it exhibits green fluorescence; if it is attached to a single-stranded nucleic acid (RNA), it emits red fluorescence. Only nonviable cells that have lost their membrane integrity and emit red fluorescence through DNA intercalation take up ethidium bromide. Based on their fluorescence emission and the physical appearance of chromatin condensation in stained nuclei, four different cell types were identified. Viable cells contain nuclei that are brilliantly green, uniform in size, and well-organized. Early apoptotic cells (those with intact membranes that have initiated DNA fragmentation) show green nuclei, while perinuclear chromatin condensation appears as vivid green patches or fragments. Late apoptotic cells have orange to red nuclei and constricted or fragmented chromatin (fig. 5 and fig. 6). Necrotic cell nuclei are uniformly orange to red in colour and lack condensed chromatin [8, 59].

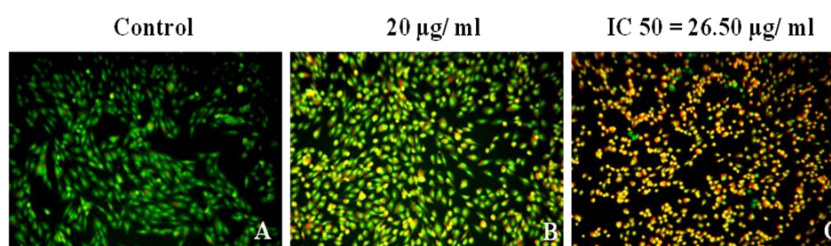


Fig. 5: Acridine orange and ethidium bromide staining (S1). A) Control, B) 20 µg/ml, C) IC 50

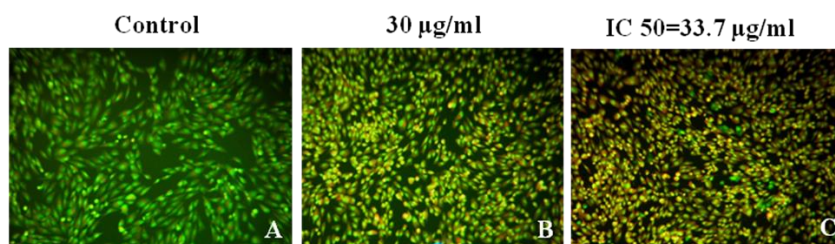


Fig. 6: Acridine orange and ethidium bromide staining (S2). A) Control, B) 20 µg/ml, C) IC 50

DISCUSSION

In their pursuit of effective cancer medicines, researchers and doctors continue to encounter a formidable obstacle [52]. Chemotherapy, radiotherapy, and individualised and targetted biological treatments are only now partially effective and almost always accompanied by significant side effects that may result in cancer recurrence with more aggressive characteristics. To address this issue, it may be necessary to increase clinical dosages of chemotherapeutic drugs to achieve greater tumor-killing effects; however, this increases drug toxicity, which is associated with a variety of undesirable side effects, such as decreased immunity and increased susceptibility to infection [53]. Numerous preclinical and clinical investigations on the efficacy of naturally occurring chemicals in the treatment of cancer have been undertaken, with some demonstrating a significant reduction in disease activity with fewer adverse effects [54]. On the other hand, the key issues are the sustainability and selectivity of naturally occurring chemicals. As a result, much effort has been devoted to the development of anti-cancer synthetic chemicals derived from naturally occurring molecules. The synthetic compounds reported here have molecular structures equivalent to those of natural drugs, include the same active components, and have far safer profiles [8].

Antibacterial, antifungal, anti-TB, and anti-cancer activities of isoniazid schiffbases have been reported [55]. Compared to zerumbone, the Isoniazid derivative (E)-N'-(2,3,4-trihydroxybenzylidene) isonicotinohydrazide (ITHB4) prevents the growth of MCF-7 breast cancer cells. ITHB4 suppressed MCF-7 tumour development with a lower IC50 than zerumbone, and an apoptosis assay demonstrated that ITHB4 triggered apoptosis and cell cycle arrest at the sub-G1 and G2/M stages in MCF-7 cells at the IC50 level. S1 and S2 can inhibit MG-63 human osteosarcoma cells at a lower cost than ITBH4, but they have the same lethal impact [8, 9].

CONCLUSION

The effects of S1 and S2 on the cell viability of MG-63 cells were determined by using the MTT cytotoxicity assay. Cells were subjected to 5-40µg/ml of each sample (S1 and S2), respectively. Both samples effectively decreased the MG-63 cell viability. Apoptosis studies confirmed this observation. However, when compared with S2, S1 showed increased cytotoxicity to the MG-63 cells with the IC50 at 26.50 µg/ml.

ACKNOWLEDGMENT

We acknowledge the Research lab-Scigen Research and Innovation Pvt. Ltd., Periyar Technology Business Incubator, Thanjavur, Tamilnadu, India for their help in apoptosis studies.

FUNDING

Nil

AUTHORS CONTRIBUTIONS

All the authors have contributed equally.

CONFLICT OF INTERESTS

The authors have no conflicts of interest.

REFERENCES

- Liu K, Liu PC, Liu R, Wu X. Dual AO/EB staining to detect apoptosis in osteosarcoma cells compared with flow cytometry. *Med Sci Monit Basic Res.* 2015 Feb 9;21:15-20. doi: 10.12659/MSMBR.893327, PMID 25664686, PMCID PMC4332266.
- Mesbah M, Douadi T, Sahli F, Issaadi S, Boukazoula S, Chafaa S. Synthesis, characterization, spectroscopic studies and antimicrobial activity of three new Schiff bases derived from Heterocyclic moiety. *J Mol Struct.* 2018 Jan;1151:41-8. doi: 10.1016/j.molstruc.2017.08.098. MOLSTRUC.2017.08.098.
- Vijayapriya M, Mahalakshmi S, Christiya CR. *In vitro* studies on antiproliferative effect of Euphorbia hirta L. Leaves. *Annals of the Romanian Society of Cell Biology.* 2021;25(4):1455-67.
- Mukherjee S, Pal CK, Kotakonda M, Joshi M, Shit M, Ghosh P. Solvent induced distortion in a square planar copper(II) complex containing an azo-functionalized schiff base: synthesis, crystal structure, *in vitro* fungicidal and anti-proliferative, and catecholase activity. *J Mol Struct.* 2021 Dec;1245:131057. doi: 10.1016/j.molstruc.2021.131057.
- RR, Shafreen M, Kumar N. Inhibition of proliferation in ovarian cancer cell line (PA-1) by the action of green compound "betanin". *Appl Biochem Biotechnol.* 2022 Jan;194(1):71-83. doi: 10.1007/s12010-021-03744-0. PMID 34762269.
- Suresh P, Xavier AS, VPK KP. Anticancer activity of cissus quadrangularis l. methanolic extract against mg63 human osteosarcoma cells- an *in vitro* evaluation using cytotoxicity assay. *Biomed Pharmacol J.* 2019;12(2):975-80. doi: 10.13005/BPJ/1724.
- Curcic MG, Stankovic MS, Mrkalic EM, Matovic ZD, Bankovic DD, Cvetkovic DM. Antiproliferative and proapoptotic activities of methanolic extracts from Ligustrum vulgare L. as individual treatment and in combination with palladium complex. *Int J Mol Sci.* 2012;13(2):2521-34. doi: 10.3390/ijms13022521. PMID 22408469, PMCID PMC3292038.
- Barathan M, Zulpa AK, Vellasamy KM, Mariappan V, Shivashkaregowda NKH, Ibrahim ZA. Cytotoxic activity of isoniazid derivative in human breast cancer cells. *In Vivo.* 2021 Sep-Oct;35(5):2675-85. doi: 10.21873/invivo.12551, PMID 34410956, PMCID PMC8408694.
- Park TS, Donnenberg VS, Donnenberg AD, Zambidis ET, Zimmerlin L. Dynamic interactions between cancer stem cells and their stromal partners. *Curr Pathobiol Rep.* 2014 Mar 1;2(1):41-52. doi: 10.1007/s40139-013-0036-5, PMID 24660130, PMCID PMC3956651.
- Narendhiran S, Mohanasundaram S, Arun J, Saravanan L, Catherine L, Subathra M. Comparative study in larvicidal efficacy of medicinal plant extracts against culex quinquefasciatus. *Int J Res Plant Sci.* 2014;4(1):22-5.
- Coleman RE. Metastatic bone disease: clinical features, pathophysiology and treatment strategies. *Cancer Treat Rev.* 2001 Jun;27(3):165-76. doi: 10.1053/ctrv.2000.0210, PMID 11417967.
- Lewis VO. What's new in musculoskeletal oncology. *J Bone Joint Surg Am.* 2009 Jun;91(6):1546-56. doi: 10.2106/JBJS.I.00375. PMID 19487537.
- Picci P, Ferrari S, Bacci G, Gherlinzoni F. Treatment recommendations for osteosarcoma and adult soft tissue sarcomas. *Drugs.* 1994 Jan;47(1):82-92. doi: 10.2165/00003495-199447010-00006, PMID 7510623.
- Bacci G, Longhi A, Versari M, Mercuri M, Briccoli A, Picci P. Prognostic factors for osteosarcoma of the extremity treated with neoadjuvant chemotherapy: 15-year experience in 789 patients treated at a single institution. *Cancer.* 2006 Mar 1;106(5):1154-61. doi: 10.1002/cncr.21724, PMID 16421923.

15. Doss VA, Mohanasundaram S, Maddisetty P. Analysis of hydroethanolic extract of *Senna alata* (L.) to screen bioactive compounds with inhibitory activity on lipid peroxidation, *in vitro* antibacterial and antidiabetic efficacy. *Int J Pharm Sci*. 2016;6(1):1360-6.
16. Stiller CA, Craft AW, Corazziari I, EURO CARE Working Group. Survival of children with bone sarcoma in Europe since 1978: results from the Eurocare study. *Eur J Cancer*. 2001 Apr;37(6):760-6. doi: 10.1016/s0959-8049(01)00004-1, PMID 11311651.
17. Liu K, Liu PC, Liu R, Wu X. Dual AO/EB staining to detect apoptosis in osteosarcoma cells compared with flow cytometry. *Med Sci Monit Basic Res*. 2015 Feb 9;21:15-20. doi: 10.12659/MSMBR.893327, PMID 25664686, PMCID PMC4332266.
18. Rangarajan N, Sampath, Dass Prakash M, Mohanasundaram S. UV Spectrophotometry and FTIR analysis of phenolic compounds with antioxidant potentials in *glycyrrhiza glabra* and *zingiber officinale*. *IJRPS* 2021;12(1):877-83. doi: 10.26452/ijrps.v12i1.4215.
19. Fletcher CDM, Unni KK. Pathology and genetics of tumours of soft tissue and bone. In: Mertens F, editor: World Health Organization Classification of tumours. Lyon, France: IARC Press; 2002.
20. Cserni G, Chmielik E, Cserni B, Tot T. The new TNM-based staging of breast cancer. *Virchows Arch*. 2018 May;472(5):697-703. doi: 10.1007/s00428-018-2301-9. PMID 29380126.
21. Arndt CA, Rose PS, Folpe AL, Laack NN. Common musculoskeletal tumors of childhood and adolescence. *Mayo Clin Proc*. 2012 May;87(5):475-87. doi: 10.1016/j.mayocp.2012.01.015. PMID 22560526, PMCID PMC3538469.
22. Rangarajan N, Sangeetha R, Mohanasundaram S, Sampath, Porkodi K, Dass Prakash MV. Additive inhibitory effect of the peels of *Citrus limon* and *Citrus sinensis* against amylase and glucosidase activity. *IJRPS* 2020;11(4):6876-80. doi: 10.26452/ijrps.v11i4.3661.
23. Al-Mosawi SK, Al-Shamkhani ZA. New heterocyclic schiff base and azetidinone as antibacterial agents. *Asian J Res Chem*. Sep 2014;7(9):801-4.
24. Kumar KS, Ganguly S, Veerasamy R, De Clercq E. Synthesis, antiviral activity and cytotoxicity evaluation of Schiff bases of some 2-phenyl quinazoline-4(3H)-ones. *Eur J Med Chem*. 2010 Nov;45(11):5474-9. doi: 10.1016/j.ejmech.2010.07.058. PMID 20724039, PMCID PMC7115544.
25. Sivakumar S, Mohanasundaram S, Rangarajan N, Sampath V, Velayutham Dass Prakash MV. *In silico* prediction of interactions and molecular dynamics simulation analysis of Mpro of severe acute respiratory syndrome caused by novel coronavirus 2 with the FDA-approved nonprotein antiviral drugs. *J Appl Pharm Sci*. 2022;12(05):104-19. doi: 10.7324/JAPS.2022.120508.
26. Shanty AA, Philip JE, Sneha EJ, Prathapachandra Kurup MR, Balachandran S, Mohanan PV. Synthesis, characterization and biological studies of Schiff bases derived from heterocyclic moiety. *Bioorg Chem*. 2017 Feb;70:67-73. doi: 10.1016/j.bioorg.2016.11.009. PMID 27894775.
27. Pontiki E, Hadjipavlou Litina D, Chaviara AT. Evaluation of anti-inflammatory and antioxidant activities of copper (II) Schiff mono-base and copper(II) Schiff base coordination compounds of dien with heterocyclic aldehydes and 2-amino-5-methylthiazole. *J Enzyme Inhib Med Chem*. 2008 Dec;23(6):1011-7. doi: 10.1080/14756360701841251, PMID 19005947.
28. Amer S, El-Wakiel N, El-Ghamry H. Synthesis, spectral, antitumor and antimicrobial studies on Cu(II) complexes of purine and triazole Schiff base derivatives. *J Mol Struct*. 2013;1049:326-35. doi: 10.1016/j.molstruc.2013.06.059.
29. Mohanasundaram S, Doss VA, HariPriya G, Varsha M, Daniya S, Madhankumar. GC-MS analysis of bioactive compounds and comparative antibacterial potentials of aqueous, ethanolic and hydroethanolic extracts of *Senna alata* L. against enteric pathogens. *Int J Res Pharm Sci*. 2017;8(1):22-7.
30. Bensaber SM, Allafe HA, Ermeli NB, Mohamed SB, Zetrini AA, Alsabri SG. Chemical synthesis, molecular modelling, and evaluation of anticancer activity of some pyrazol-3-one Schiff base derivatives. *Med Chem Res*. 2014;23(12):5120-34. doi: 10.1007/s00044-014-1064-3.
31. Sinha A, Banerjee K, Banerjee A, Das S, Choudhuri SK. Synthesis, characterization and biological evaluation of a novel vanadium complex as a possible anticancer agent. *J Organomet Chem*. 2014;772-773:34-41. doi: 10.1016/j.jorganchem.2014.08.032.
32. Wang Q, Sivakumar K, Mohanasundaram S. Impacts of extrusion processing on food nutritional components. *Int J Syst Assur Eng Manag*. 2022;13(S1):364-74. doi: 10.1007/s13198-021-01422-2.
33. Qin W, Long S, Panunzio M, Biondi S. Schiff bases: a short survey on an evergreen chemistry tool. *Molecules*. 2013 Oct 8;18(10):12264-89. doi: 10.3390/molecules181012264, PMID 24108395, PMCID PMC6270622.
34. Mohanasundaram S, Rangarajan N, Sampath V, Porkodi K, Pennarasi M. GC-MS and HPLC analysis of antiglycogenolytic and glycogenic compounds in kaempferol 3-O-gentiobioside containing *Senna alata* L. leaves in experimental rats. *Translational Metab Syndr Res*. 2021;4:10-7.
35. Uddin E, Islam R, Bitu NA, Hossain S, Uddin N. Biological applications of isoniazid derived Schiff base complexes: an overview. *Asian J Res Biochem*. 2020;6(3):17-31. doi: 10.9734/AJRB/2020/v6i330118.
36. Rodrigues FA, Oliveira AC, Cavalcanti BC, Pessoa C, Pinheiro AC, de Souza MV. Biological evaluation of isoniazid derivatives as an anticancer class. *Sci Pharm*. 2014;82(1):21-8. doi: 10.3797/scipharm.1307-25, PMID 24634839, PMCID PMC3951230.
37. de Souza MV. Current status and future prospects for new therapies for pulmonary tuberculosis. *Curr Opin Pulm Med*. 2006 May;12(3):167-71. doi: 10.1097/01.mcp.0000219264.42686.c9. PMID 16582670.
38. Keri RS, Sasidhar BS, Nagaraja BM, Santos MA. Recent progress in the drug development of coumarin derivatives as potent antituberculosis agents. *Eur J Med Chem*. 2015 Jul 15;100:257-69. doi: 10.1016/j.ejmech.2015.06.017. PMID 26112067.
39. Black M, Hussain H. Hydrazine, cancer, the internet, isoniazid, and the liver. *Ann Intern Med*. 2000 Dec 5;133(11):911-3. doi: 10.7326/0003-4819-133-11-200012050-00016, PMID 11103062.
40. Doss VA, Maddisetty P, Mohanasundaram S. Biological active compounds with various medicinal values of *strychnos nuxvomica*-a pharmacological summary. *J Glob Trends Pharm Sci*. 2016;7(1):3044-7.
41. Berkesi O, Kortvelyesi T, Hetenyi C, Nemeth T, Palinko I. Hydrogen bonding interactions of benzylidene type Schiff bases studied by vibrational spectroscopic and computational methods. *Phys Chem Chem Phys*. 2003;5(10):2009-14. doi: 10.1039/B301107K.
42. Yong J, Mainsah E, Ntumu S, Ndifon P. Synthesis, characterization and antibacterial studies of some isoniazid-derived schiff bases. *IRJPAC* 2016;12(1):1-8. doi: 10.9734/IRJPAC/2016/27100.
43. Rodrigues FA, Oliveira AC, Cavalcanti BC, Pessoa C, Pinheiro AC, de Souza MV. Biological evaluation of isoniazid derivatives as an anticancer class. *Sci Pharm*. 2014;82(1):21-8. doi: 10.3797/scipharm.1307-25, PMID 24634839, PMCID PMC3951230.
44. Cheng J, Wang X, Qiu L, Li Y, Marraiki N, Elgorban AM. Green synthesized zinc oxide nanoparticles regulates the apoptotic expression in bone cancer cells MG-63 cells. *J Photochem Photobiol B*. 2020 Jan;202:111644. doi: 10.1016/j.jphotobiol.2019.111644. PMID 31770706.
45. Karthikeyan V, Sivakumar K, Gokuldass A, Mohana Sundaram S. Studies on larvicidal activity of *leucas aspera*, *vitex negundo* and *eucalyptus* against *culex quinquefasciatus* collected from coovum river of Chennai, India. *Asian J Pharm Sci Clin Res*. 2012;5(3):1-4.
46. Gherghi ICh, Girousi ST, Voulgaropoulos AN, Tzimou Tsitouridou R. Study of interactions between DNA-ethidium bromide (EB) and DNA-acridine orange (AO), in solution, using hanging mercury drop electrode (HMDE). *Talanta*. 2003 Oct 17;61(2):103-12. doi: 10.1016/S0039-9140(03)00238-8, PMID 18969168.

47. Leite M, Quinta Costa M, Leite PS, Guimaraes JE. Critical evaluation of techniques to detect and measure cell death-study in a model of UV radiation of the leukaemic cell line HL60. *Anal Cell Pathol.* 1999;19(3-4):139-51. doi: 10.1155/1999/176515, PMID 10866276.
48. Mohanasundaram S, Rangarajan N, Sampath V, Porkodi K, Dass Prakash MV, Monicka N. GC-MS identification of anti-inflammatory and anticancer metabolites in edible milky white mushroom (*Calocybe indica*) against human breast cancer (MCF-7) cells. *Res J Pharm Technol.* 2021;14(8):4300-6.
49. Ramadevi P, Singh R, Prajapati A, Gupta S, Chakraborty D. Cu(II) complexes of isoniazid schiff bases: DNA/BSA binding and cytotoxicity studies on A549 cell line. *Adv Chem.* 2014. doi: 10.1155/2014/630575.
50. Bharathi P, Elavarasi N, Mohanasundaram S. Studies on rate of biodegradation of vegetable oil (Cocunut oil) by using *Pseudomonas* sp. *Int J Environ Biol.* 2012;2(2):12-9.
51. Baskic D, Popovic S, Ristic P, Arsenijevic NN. Analysis of cycloheximide-induced apoptosis in human leukocytes: fluorescence microscopy using annexin V/propidium iodide versus acridin orange/ethidium bromide. *Cell Biol Int.* 2006 Nov;30(11):924-32. doi: 10.1016/j.cellbi.2006.06.016. PMID 16895761.
52. Ujjan JA, Morani W, Memon N, Mohanasundaram S, Nuhmani S, Singh BK. Force platform-based intervention program for individuals suffering with neurodegenerative diseases like Parkinson. *Comput Math Methods Med.* 2022. doi: 10.1155/2022/1636263, PMID 35082910.
53. Hosseini A, Ghorbani A. Cancer therapy with phytochemicals: evidence from clinical studies. *Avicenna J Phytomed.* 2015 Mar-Apr;5(2):84-97. PMID 25949949, PMCID: PMC4418057.
54. Mohanasundaram S, Victor Arokia Doss VA, Prasad Maddisetty P, Magesh R, Sivakumar K, Subathra M. Pharmacological analysis of hydroethanolic extract of *Senna alata* (L.) for *in vitro* free radical scavenging and cytotoxic activities against Hep G2 cancer cell line. *Pak J Pharm Sci.* 2019;32(3):931-4.
55. Cui J, Jing W, Guo S, Cui J, Zhou M. *Triphala* suppresses ovarian cancer cell proliferation through induction of apoptosis and ROS *in vitro*. *International Journal of Pharmacology.* 2021;17(7):491-8. <https://doi.org/10.3923/ijp.2021.491.498>.
56. Vijayalakshmi A, Sindhu G. Umbelliferone arrest cell cycle at G0/G1 phase and induces apoptosis in human oral carcinoma (KB) cells possibly via oxidative DNA damage. *Biomed Pharmacother.* 2017 Aug;92:661-71. doi: 10.1016/j.biopha.2017.05.128. PMID: 28586740.